Cement & Concrete Composites 32 (2010) 204–210

Contents lists available at ScienceDirect

Cement & Concrete Composites

journal homepage: www.elsevier.com/locate/cemconcomp

The effect of processed fly ashes on the durability and the corrosion of steel rebars embedded in cement–modified fly ash mortars

P. Garcés [a,*], L.G. Andión [a], E. Zornoza [b], M. Bonilla [b], J. Payá [b]

[a] Dpto. Ing. de la Construcción, Obras Públicas e Infr. Urb. Univ., Alicante. Apdo. Correos 99, 03080 Alicante, Spain
[b] Grupo de Investigación en Química de los Materiales de Construcción GIQUIMA, Instituto de Ciencia y Tecnología del Hormigón ICITECH, Univ. Politécnica de Valencia, Spain

ARTICLE INFO

Article history:
Received 1 June 2007
Received in revised form 7 April 2009
Accepted 12 November 2009
Available online 18 November 2009

Keywords:
Processed fly ashes
Chlorides
Migration
Corrosion

ABSTRACT

This paper deals with the study of corrosion level of reinforcing steel bars embedded in Portland cement mortars containing different types of fly ash. Fly ashes used were obtained by physico-chemical treatments of an original F class fly ash to modify their magnetic properties and reduce their particle size. An original fly ash (T0) and three types of modified ashes were tested according to treatment duration and magnetic properties (T60, ground fly ash; TNM, non-magnetic fraction; TM, magnetic fraction). Corrosion tests on reinforced mortar specimens with and without different types of fly ashes, cured at 40 °C, and under accelerated carbonation conditions and seawater immersion, have been performed in order to obtain conclusions on durability. From the corrosion point of view the addition of TNM in mortars showed to be much more effective than addition of the original T0 fly ash.

1. Introduction

Generally speaking, the utilization of fly ash in concrete and mortar production brings economic benefits because it is usually a low-cost material and it can be used to replace higher-cost materials [1]. Additionally, in some cases, the use of fly ash in concrete and mortar mixes represents technological advantages, due to pozzolanic activity, workability of mixes and regularity of production and composition. Finally, environmental aspects should be taken into account when fly ash is used: for example, energy saving, reduction of carbon dioxide emission, and lessened disposal problems [2–5]. More questions and factors arise when trying to make these materials applicable to reinforced concrete structures because the protection of rebars from corrosion is essential.

At present, there are some references in the specialised bibliography concerning the corrosion levels of reinforcing steel embedded in these cement–fly ash mortar and concrete mixes [6–21]. The majority of research works assert that ash additions affect positively (less corrosion) the rebar corrosion state in the presence of chloride ions [12,13,15–18,20,21], whereas other authors maintain that such additions have a negative effect under carbonation conditions [14,19]. The beneficial effects on chloride-induced corrosion are mainly related to the reduction in the permeability properties of the cementing matrix, due to the improvement in the workability and the densification by the pozzolanic reaction. Obviously, the pozzolanic effect of fly ash can reduce the alkaline reserve of concrete and a reduction of the carbonation resistance of the concrete cover is observed.

Some particles of fly ash have the ability to interact with a magnetic field, while some others do not have this property due to a different proportion of iron oxides in each individual particle. The influence of the different fly ash fractions, in terms of their different magnetic behaviour, on the corrosion of reinforcing steel has not been previously reported. Several studies on alternative procedures for modifying the nature of fly ash samples have been presented [22–27]. The spherical particles are broken down by mechanical grinding and consequently the fineness and pozzolanic reactivity is significantly increased. With the magnetic-extraction treatment, an examination of particles where the spherical shape is maintained provides fly ash fractions, magnetic and non-magnetic, differing in chemical composition.

An important research effort has been dedicated to analyse and interpret the influence of this type of ash when used in the fabrication of mortar and concrete mixes [22–27]. These studies however have concentrated on the changes that the presence of ashes produces in the properties of such mixes: workability, compressive and flexural strengths, and lime fixation. This could be sufficient for mass concrete constructions but the most used material in construction is reinforced concrete in which there is another material that must be taken into account: the reinforcing steel.

The main objective of the present paper is to study the effect of modifying the nature of fly ash samples on the corrosion rates of reinforcing steel embedded in cement–modified fly ash mortars.

* Corresponding author. Tel.: +34 965903707; fax: +34 965903678.
E-mail address: pedro.garces@ua.es (P. Garcés).

0958-9465/$ - see front matter © 2009 Elsevier Ltd. All rights reserved.
doi:10.1016/j.cemconcomp.2009.11.006

2. Experimental programme

2.1. Materials and specimen preparation

Low-calcium fly ash (class F according to ASTM C-618) from the thermoelectric power plant Andorra-Teruel (Spain) was used to obtain the various fractions of modified fly ashes: T0, original fly ash; T60, original fly ash ground for 60 min; TM, magnetic fraction of the original fly ash; and TNM, non-magnetic fraction of the original fly ash. Fly ash chemical compositions are summarized in Table 1. Cement type CEM I 42.5R (OPC) meeting the Spanish standard [28] requirements was used. Silica sand (of standard particle size distribution) and distilled water were always employed. The mortar combined one part (by mass) of cement and three parts of sand. Different mortars were prepared using 0.5 and 0.7 w/c (water/cement + fly ash ratio), and replacing 30% of cement by fly ash (by mass). The specimens for corrosion tests were prismatic $2 \times 5.5 \times 8$ cm and contained, embedded, two identical bars of carbon steel (∅6 mm). A graphite bar embedded in the middle was used as a counter-electrode. The resulting thickness of the mortar cover for the electrodes was 7 mm. The mortar specimens were prepared in the laboratory at 20 °C and 80% R.H. After demoulding, 24 h later, test specimens were immersed in water for 28-days of curing period at 40 °C, to ensure that pozzolanic reaction was well advanced.

For migration tests cylindrical mortar specimens (10 cm diameter, 12 cm height) were prepared. After hardening, specimens were submerged in water for a 28-day curing period. Then, two discs (10 cm diameter, 15 mm thickness) were extracted from each specimen. These discs were the samples to be tested in the chloride migration tests. The values presented in this work are the mean value of these two replicates of each specimen. Prior to the performance of the tests, the samples were water saturated in order to eliminate the air in the pores.

In the process of carbonation the test specimens were maintained in a chamber holding a 100% CO_2 atmosphere at a RH of ≅65% [30], in order to achieve a rapid carbonation. Prismatic specimens (of 2 cm × 2 cm × 8 cm dimensions) of the prepared mortars were also stored in the chamber and were used to control the carbonation front progress.

On the other hand, for the seawater attack tests, specimens were partially submerged in seawater, see Fig. 1. The immersion depth was 7 cm to avoid the contact between the external part of the steel electrodes and the solution.

Natural Mediterranean seawater was used in corrosion experiments, with ion content as summarized in Table 2.

Standard corrugated steel rebars were used for the experiment. The steel exposed area was 9 cm^2. Bars were previously cleaned in $HCl:H_2O$ 1:1 with urotropine solutions, abraded with abrasive paper, and degreased in acetone. Adhesive tape, tightly pressed, was used to limit the exposed area.

2.2. Extraction procedures

Original fly ash (T0) was suspended in water and mechanically and vigorously stirred. Maintaining the stirring, a hand electromagnet with a plastic shelter was introduced in the suspension for 30 s and then removed. Fly ash magnetic fraction (TM) adhered to the plastic surface and, when the current was switched off, the magnetic fraction was obtained. This process was repeated several times, until the amount of adhered fly ash was negligible. Non-extracted fly ash (that is, the non-magnetic fraction, TNM) and TM fraction were heated at 110 °C for 24 h, yielding two dried fly ash samples, ready for experiments.

Table 1
Chemical composition of original and modified fly ashes [29].

Fly ash	SiO_2	Fe_2O_3	Al_2O_3	CaO	MgO	LOI[a]
T0/T60	41.40	15.95	26.22	6.10	1.11	2.20
TM	28.7	24.3	34.4	7.4	1.5	0.5
TNM	42.5	5.6	31.4	11.7	2.0	1.8

[a] LOI: loss on ignition.

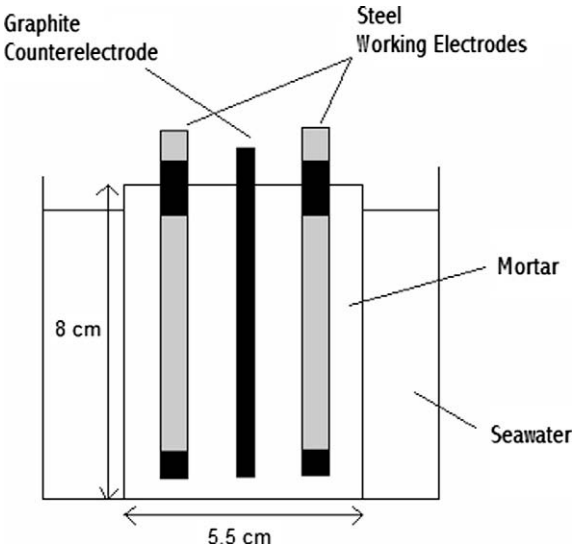

Fig. 1. Cross section view of the specimen partially submerged in seawater.

Table 2
Ion content of sea water used in the experiments.

Ion	Na^+	K^+	Ca^{2+}	Mg^{2+}	Cl^-	SO_4^{2-}	HCO_3^-
mg/l	12,000	400	450	1500	21,500	2900	130

2.3. Grinding procedure

Samples of original fly ash (T0) were ground using a laboratory ball-mill (Gabbrielli Mill-2) for 60 min: 450 g of T0 were introduced into the bottle mill containing 80 alumina balls (18 mm in diameter). The ground sample was designated T60.

2.4. Scanning electron microscopy (SEM)

The scanning electron microphotographs were taken with a JEOL JSM-6300 SEM equipped with an energy dispersive X-ray (EDX) analyser. High vacuum evaporation was used to deposit a thin gold film to make the specimen surfaces electrically conductive.

2.5. Corrosion measurement technique

The electrochemical technique used to measure the instantaneous corrosion rate, I_{corr}, was the polarization resistance technique, through the well known Stern–Geary formula [31] $I_{corr} = B/R_p$. I_{corr} was calculated assuming values of $B = 26$ mV for corroding steel or 52 mV for passive steel. R_p and corrosion potential (E_{corr}) were periodically measured during the time of the experiment, and also the weight loss was measured, for each electrode, at the end of the test. All potentials are referred to saturated-calomel electrode (SCE). A potentiostat–galvanostat EG&G Model 362 was used. I_{corr} data were calculated as average values of four

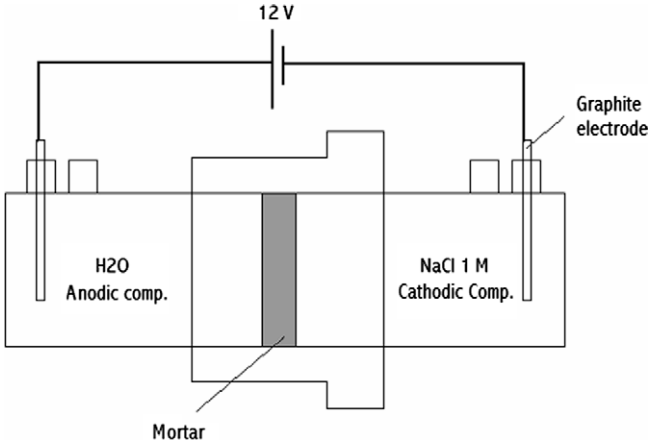

Fig. 2. Experimental arrangement used in migration tests.

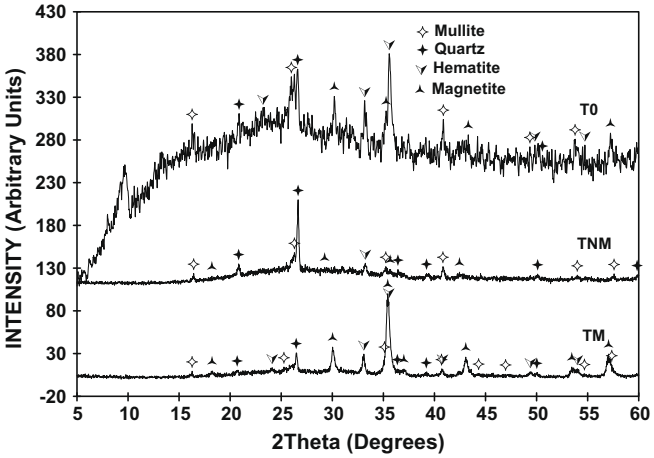

Fig. 3. X-ray diffraction plots of the fly ash fractions.

measurements (two specimens, two electrodes each). After the corrosion tests were performed, mortar specimens were broken and the steel electrodes were extracted. These electrodes were cleaned and weighted to compare the electrochemical mass loss (calculated by integrating the I_{corr} vs. time graph and applying Faraday's law) with the gravimetric mass loss (obtained by the difference between initial and final mass of steel electrodes). The good agreement obtained between the two weight loss values validates the B values employed.

2.6. Migration tests

To perform the steady-state migration tests, a two compartment cell as shown in Fig. 2 was used. This arrangement had been previously and successfully used by Castellote et al. [32] to obtain steady and non-steady chloride diffusion coefficients. The mortar sample was placed in the migration cell separating the cell in two chambers. Distilled water was introduced in the compartment where the anode was located (anolyte) in all cases. The voltage applied was 12 V DC, although the real voltage drop across the specimen was measured as indicated in Ref. [33]. Periodically in the course of the experiment the electrical field was switched off and, after waiting for 5 s, the conductivity of the anodic solution was measured by introducing a conductive electrode in the compartment. Conductivity values were referenced at 25 °C. Once the conductivity was recorded, the electrical field was switched on again to continue the test. Conductivity values were transformed to chloride concentration ones using the relation found by Castellote et al. [32]:

$$[Cl^-]\ (mM) = -1.71 + 11.45 \cdot \rho\ (mS/cm)$$

3. Results and discussion

3.1. Characterisation of fly ash fractions

The classification of fly ashes using magnetic procedures, such as extraction using hand-magnets or hand-electromagnets, logically leads to fractions with essentially different content in iron compounds. When the original fly ash T0 was divided in magnetic TM and non-magnetic TNM fractions, a noteworthy difference in iron content occurs (see Table 1), giving a very high iron oxide content, higher than 24%, for the TM fraction. This is attributed to the presence of a high amount of magnetite. X-ray diffractograms for T0, TNM and TM fly ashes are shown in Fig. 3. It can be noted that in curve for TNM, main mineral phases were quartz and mullite, whereas TM sample showed additionally peaks for magnetite and hematite. Additionally TM fly ash fraction was very coarse (see Fig. 4 and Table 3). On the other hand, T60 and TNM contained the highest volume of particles under 10 μm in diameter (67.01% and 42.00% respectively) and are considered finer than T0.

Fig. 5 shows some SEM photos of different types of fly ash particles. Micrographs, Fig. 5a, c and d, show the typical spherical and spheroidal shaped particles of fly ashes. The magnetic extraction procedure did not change the particle shape. On the other hand, micrograph, Fig. 5b, shows that original fly ash particles have been broken, however some remaining spherical small particles are also observed.

3.2. Corrosion and migration results

The effect in rebar corrosion of the addition in mortar samples of the four types of fly ashes (T0, T60, TNM and TM), made with 0.5 w/c ratio, cured for 28 days at 40 °C and 100% RH, and subjected to the following two conditions has been studied: chloride and migration attacks, which are the typical agents causing durability problems.

3.2.1. Partial immersion in seawater: corrosion studies

After the curing period (28 days, RH = 100%, 40 °C), water-saturated samples (two for each fly ash type) were partially immersed

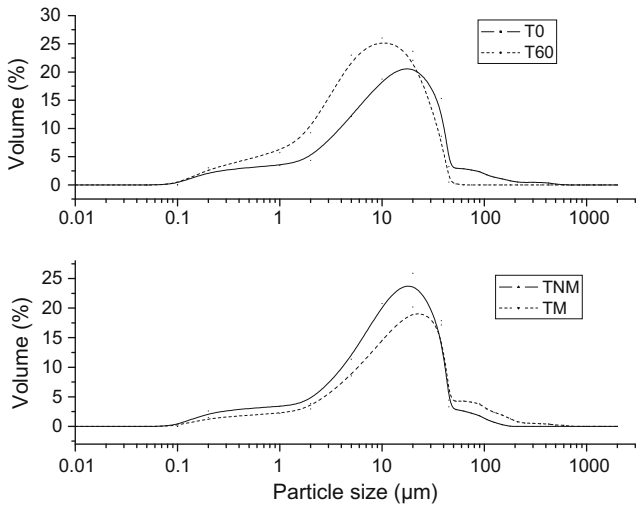

Fig. 4. Particle size distribution of the fly ash fractions.

Table 3
Selected characteristic parameters of the fly ash fractions.

Fly ash type	Mean diameter (μm)	$D[0.1]$ (μm)	$D[0.5]$ (μm)	$D[0.9]$ (μm)	Volume under 45 μm (%)	Volume under 10 μm (%)
T0	30.09	1.90	13.04	73.01	81.94	41.28
T60	8.73	1.13	6.46	19.46	99.82	67.01
TNM	20.05	2.04	12.32	49.38	88.35	42.00
TM	40.13	3.23	20.02	96.64	73.23	30.73

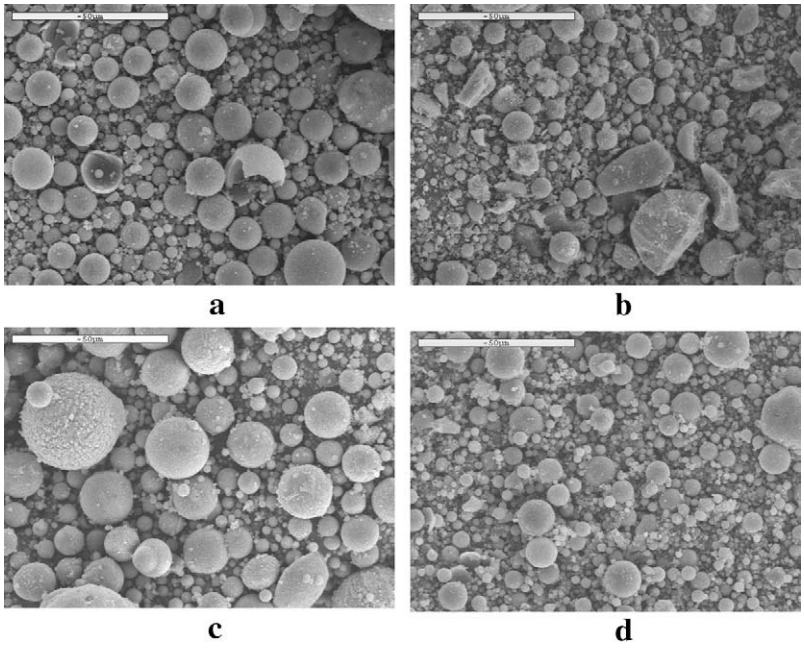

Fig. 5. SEM photos of different types of fly ash particles: (a) original, T0; (b) ground sample, T60; (c) magnetic fraction, TM; (5): non-magnetic fraction, TNM.

in seawater, being the immersion depth 7 cm to avoid the contact between the seawater and the external part of the rebars. In these experiments two specimens with w/b = 0.7 and 0.5 were also tested in order to compare for different porosity values and use the similar water/cement ratio as in fly ash-containing mortar (that is considering fly ash as an addition). From the beginning of this test phase significant differences in corrosion behaviour were observed for rebars embedded in each of the mortar samples.

The transition between currents of 0.1 and 0.2 μA/cm^2, as marked in Fig. 6, corresponds approximately to the transition to a regime of active corrosion, in terms of decrease of service life and a tolerable corrosion rate [34].

Initially, prior to seawater immersion, all samples presented relatively high corrosion intensity values, between 0.2 μA/cm^2 and 0.9 μA/cm^2 (Fig. 6). However, during the next 28 days the corrosion rate decreased progressively down to values between 0.03 μA/cm^2 and 0.07 μA/cm^2. This initial high corrosion rate taking place at the beginning of the test is due to the passivation process, since passivation involves the corrosion of the steel surface [14,35,36].

After seawater immersion, differences became quite considerable by the end of the experiment, between 180 and 190 days, at which point the corrosion intensity profile has reached a stationary value, which is different for each of the samples. The highest corrosion intensity values correspond to rebars embedded in mortar without additions and w/c ratio of 0.7: their values increased from an initial 0.04 μA/cm^2 to a stationary value of about 1.7 μA/cm^2.

Substitution of 30% of cement mass by ground fly ash (T60) and non-magnetic fly ash (TNM) leads to a significant improvement in rebar corrosion protection in this particularly aggressive environment. Steels embedded in mortars with original fly ash (T0) and magnetic fraction of fly ash (TM) offered corrosion rates slightly higher than steels embedded in the control mortar with w/c = 0.5, although lower than steels embedded in control mortar with w/c = 0.7.

The corrosion intensity values detected in rebars embedded in T0 added mortars were among the highest registered in modified fly ash added mortars: they increased from an initial 0.07 μA/cm^2 up to a stationary value of about 1 μA/cm^2. Next is the TM fly ash sample, showing high corrosion intensity values with a mean value of about 0.3 μA/cm^2. Probably the reason for the behaviour of the TM containing mortar is the low pozzolanic reaction degree for this type of fly ash; consequently, chloride ions diffuse more easily in this matrix. However, T0 fly ash is considered much more reactive but the corrosion rate was significant: probably, the presence of large porous carbon particles [37] for this matrix did not improve the barrier effect to chloride diffusion. Values below 0.1–0.2 μA/cm^2 are considered to mean negligible corrosion levels, not significantly affecting the service life expectancy of the structure. These low values were found for T60 and TNM containing mortars. In these cases, their high pozzolanic activity [24–26] and the fineness of carbon particles (despite that the T60 ignition loss value is higher than the T0 one) could be the responsible of the denser developed matrices acting as barriers to chloride diffusion. The lowest values of corrosion intensity among all studied cases correspond to rebars embedded in OPC mortars added with the TNM fraction of fly ash, showing a stationary value of about 0.01 μA/cm^2.

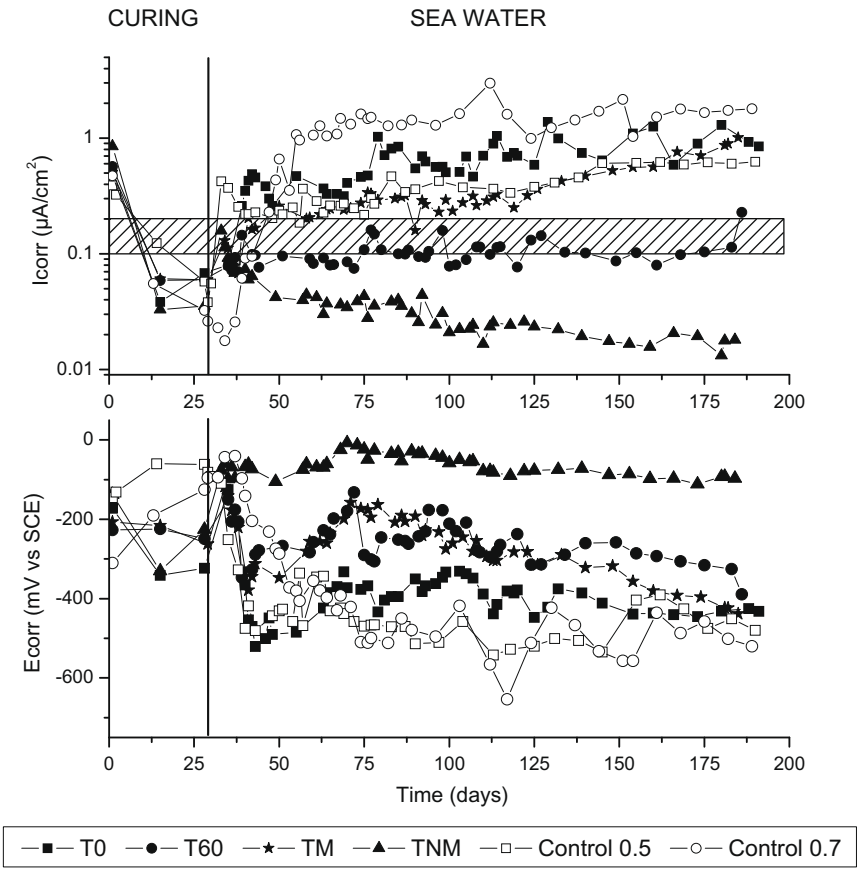

Fig. 6. Evolution of I_{corr} and E_{corr} with time for mortar samples cured for 28 days, at 40 °C and 100% RH, and subjected to seawater immersion.

In the lower part of Fig. 6 open circuit potential (OCP) values of steel using a saturated-calomel electrode are presented. It can be observed that steel bars with higher I_{corr} values offered lower E_{corr}, indicating the effective depassivation of the steel electrodes due to the increase in the chloride concentration at the steel surface. The electrodes in mortars with non-magnetic fly ash were not affected by the immersion in the chloride solution, since no increase of their corrosion rate or decrease of their corrosion potential was observed, indicating that the chloride quantity arriving to the steel surface was not high enough to depassivate the electrode.

From these results it can be inferred that the use of TNM and T60 modified fly ash additions for OPC mortars cured for 28 days at 40 °C and subjected to seawater immersion, is clearly beneficial from the point of view of corrosion, producing a decrease in the registered I_{corr} values, TNM being the best.

3.2.2. Chloride migration tests

Fig. 7 shows the evolution of chloride concentration in the anolyte for mortars: chlorides appear in the anodic compartment following the order: control, TM and T0, and finally, T60 and TNM. This can be more accurately summarised in non-steady-state diffusion coefficients (D_{ns}) (Table 4) that are derived from the time lag until the chloride concentration achieves breakthrough into the anodic compartment.

Table 4 also shows steady-state diffusion coefficient (D_s) values that have been obtained through the slopes in the chloride concentration graphs of Fig. 7; the same above mentioned order of merit can be observed for steady-state diffusion.

These results can be related to I_{corr} measurements, Fig. 6, where corrosion rate was monitored while specimens were submerged in seawater. D_s is a parameter that mainly affects corrosion in the

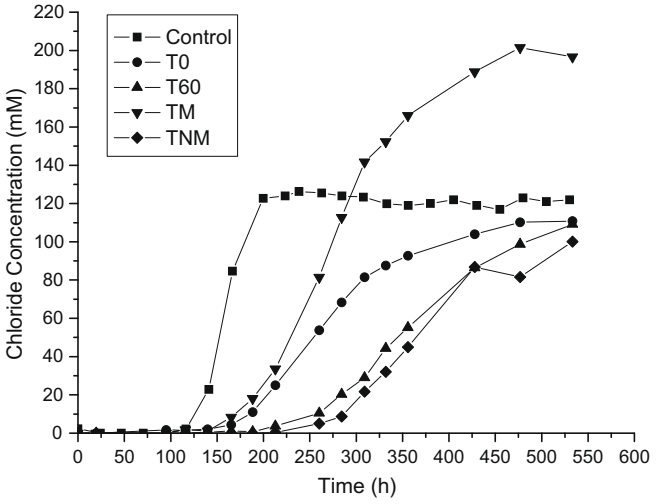

Fig. 7. Evolution of chloride concentration in the anodic compartment in migration experiments.

Table 4
Steady and non-steady-state chloride diffusion coefficient for mortars.

Mortar type	D_{ns} (m^2/s)	D_s (m^2/s)
Control	8.06×10^{-12}	5.99×10^{-12}
T0	2.31×10^{-12}	2.02×10^{-12}
T60	1.71×10^{-12}	1.26×10^{-12}
TM	2.73×10^{-12}	3.83×10^{-12}
TNM	1.78×10^{-12}	1.65×10^{-12}

propagation period because it shows the rate of chloride ingress in the mortar. The trends of both the corrosion level and the steady-state chloride diffusion coefficient are similar, but do not duplicate exactly, because other factors not considered in these tests, such as oxygen diffusion through the mortar, can affect the corrosion process .

3.2.3. Carbonation of specimens: corrosion studies

All concrete structures, especially those exposed to atmospheric conditions, are subjected to a concrete neutralization process. Due to the highly alkaline character of concrete, it reacts with atmosphere agents (usually acid substances) or neutral aqueous media (potable or seawater). In the first case SO_2 and CO_2 are responsible for such neutralization, whereas in aqueous media, the dissolved carbonic acid along with leaching process, are mainly affecting the paste alkaline phases ($Ca(OH)_2$). Fly ashes with different particle size values have demonstrated [19] that the reduction of particle size yields an increase of both reactivity with water and acid neutralization capacity.

The initial corrosion rate values obtained at one day curing time, see Fig. 8, are relatively low for all samples, between 0.05 μA/cm^2 and 0.4 μA/cm^2. During the curing period, 28 days, all corrosion rate values decrease, finally reaching similar values between 0.005 μA/cm^2 and 0.02 μA/cm^2.

Once the curing period was completed, the samples were rapidly carbonated under accelerated conditions: 100% CO_2 and 65% of RH. In this way the carbonation front reaches the steel surface very quickly. Initially an important increase of the I_{corr} values was detected. From the very beginning significant behaviour differences were observed regarding the corrosion of rebars embedded in different mortar types. Thus, a clear distinction in the behaviour was noticed between TM and TNM fraction added samples, very similar to each other, in comparison to the original ash (T0) added samples and to the one with 60 min milled (T60), which in turn had a similar behaviour by the end of the carbonation phase. Steel bars embedded in mortars with TM and TNM reach steady I_{corr} values around 0.3 μA/cm^2, and steel bars embedded in T0 and T60 show corrosion rates around 0.5 μA/cm^2. Although all steel bars are clearly depassivated, as a consequence of the carbonation of the mortar cover, there exists minor differences of TM and TNM with respect to T0 and T60. Since carbonation conditions are very aggressive, it is not possible to evaluate the carbonation resistance of the mortars. In the lower part of Fig. 8, E_{corr} evolution of steels is presented. The trends observed for all steel bars are almost identi-

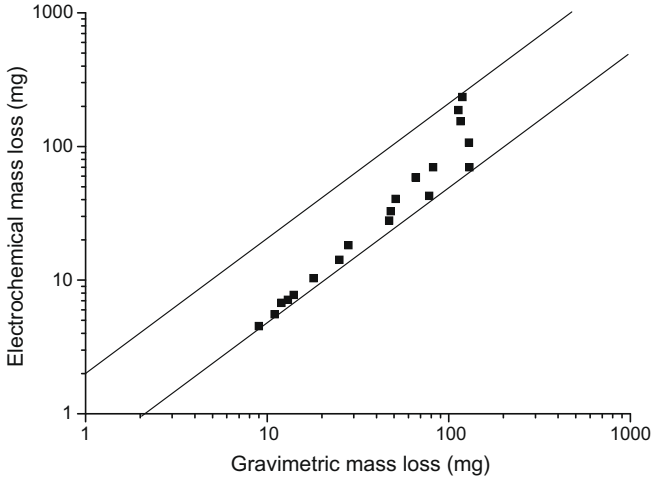

Fig. 9. Comparison between electrochemical and gravimetric mass losses in mortar specimens.

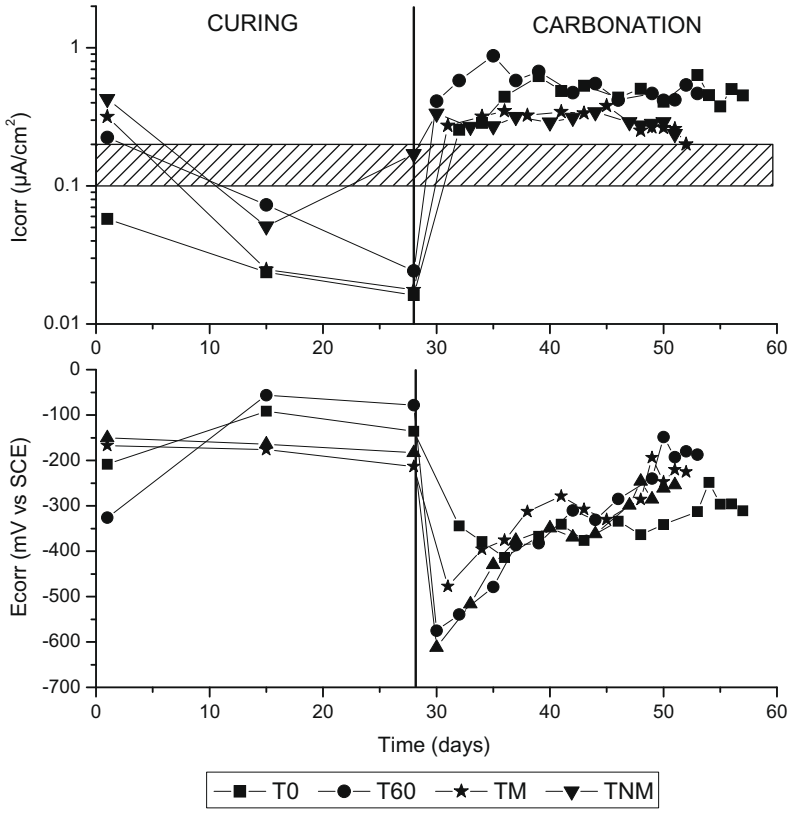

Fig. 8. Evolution of I_{corr} with time for mortar samples cured for 28 days, at 40 °C and 100% RH, and subjected to carbonation.

cal meaning that the behaviour of these mortars under carbonation conditions is very similar.

3.3. Checking with the gravimetric losses

The electrochemical loss (from R_p measurements) vs. gravimetric losses are presented in the Fig. 9. It can be observed that all points lie inside the error factor of two reported by Stern and Geary [31] for R_p measurements. Therefore, the assumed B values (26 mV) may be considered correct.

4. Conclusions

1. Processing fly ashes by magnetic extraction or by grinding yields certain types of material showing differences in particle size distribution, chemical composition and reactivity, as documented in previous papers [24–26]. In general, significant differences in corrosion behaviour of steel rebars embebded in the mortar containing these processed fly ash types have been observed.
2. Mortars containing the lowest pozzolanic reactivity ash [26], that is the magnetic fraction TM, showed the poorest corrosion protection of embedded rebars in aggressive chloride medium.
3. From the steel corrosion point of view, TNM and T60 additions were more effective than T0 addition when mortars are cured at 40 °C, under chloride aggressive medium.
4. Chloride migration tests have shown that grinding fly ashes and removing the magnetic fraction can improve the chloride ingress resistance of mortars.
5. For carbonated samples, TNM and TM fly ash mortars showed a slightly better behaviour from the steel rebar corrosion point of view.

Acknowledgements

GIQUIMA thanks to Microscopy Services of the Polytechnic University of Valencia for SEM studies, and DGICYT Spain (Project PB-93-0384) and Generalitat Valenciana (Grupos UNICH) for financial support. Authors thank Prof. F.P. Glasser his comments on this paper.

References

[1] Metha PK. Concrete structure properties and materials. New Jersey: Prentice-Hall, Inc., Englewood Cliffs; 1986. p. 1–449.
[2] Taylor HFW, editor. Cement chemistry. San Diego: Academic Press Inc.; 1990. p. 1–382.
[3] Wesche K, editor. Fly ash in concrete: properties and performance. Rilem Report 7. London: Chapman & Hall; 1991.
[4] Alonso MC, de Luxán MP, editors. Aplicaciones de las cenizas volantes en el campo de la construcción. Experiencia española. Spain: ASINEL and IETCC (CSIC); 1995.
[5] Malhotra VM. Durability of concrete incorporating high-volume of low-calcium (ASTM class F) fly ash. Cem Concr Compos 1990;12:271–7.
[6] Cabrera JG, Ghoddoussi. The influence of fly ash on the resistivity and rate of corrosion of reinforced concrete. Durability of concrete (CANMET/ACI) SP-145-12; 1994. p. 229–44.
[7] Al-Almoudi OSB et al. Carbonation and corrosion of rebars in salt contaminated OPC/PFA concretes. Cem Concr Res 1991;21:38–50.
[8] Andrade C. Effect of fly ash in concrete on the corrosion of steel reinforcement. Fly ash, silica fume, slag and natural pozzolans in concrete (CANMET/ACI), vol. 2 (91–28); 1986. p. 609–20.
[9] Haque MN, Kawamura M. Carbonation and chloride induced corrosion of reinforcement in fly ash concretes. ACI J Mater 1992;10:41–8.
[10] Gonzalez JA, Alonso C, Andrade C. Corrosion rate of reinforcements during accelerated carbonation of mortar made with different type of cements. Corrosion of reinforcement in concrete construction. SCI; 1983. p. 159–74 [chapter 11].
[11] Page CL, Short NR, Holden WR. The influence of different cements on chloride induced corrosion of reinforcing steel. Cem Concr Res 1989;16:79–86.
[12] Andrade C, Alonso C, Goñi S, Bacle B. Five years study of rebar corrosion in concrete fabricated with blended cements immersed in natural sea water. Blended cements in construction. Elsevier Applied Science; 1991. p. 429–41.
[13] Koulombi N, Batis G. Chloride corrosion of steel rebars in mortars with fly ash admixtures. Cem Concr Compos 1992;14:199–207.
[14] Zornoza E, Payá J, Garcés P. Chloride-induced corrosion of steel embedded in mortars containing fly ash and spent cracking catalyst. Corros Sci 2008;50:1567–75.
[15] Miranda JM, Fernández-Jiménez A, González JA, Palomo A. Corrosion resistance in activated fly ash mortars. Cem Concr Res 2005;35:1210–7.
[16] Chindaprasirt P, Rukzon S. Strength, porosity and corrosion resistance of ternary blend Portland cement, rice husk ash and fly ash mortar. Constr Build Mater 2008;22:1601–6.
[17] Kayali O, Zhu B. Chloride induced reinforcement corrosion in lightweight aggregate high-strength fly ash concrete. Constr Build Mater 2005;19:327–36.
[18] Saraswathy V, Muralidharan S, Thangavel K, Srinivasan S. Influence of activated fly ash on corrosion-resistance and strength of concrete. Cem Concr Compos 2003;25:673–80.
[19] Montemor MF, Cunha MP, Ferreira MG, Simoes AM. Corrosion behaviour of rebars in fly ash mortar exposed to carbon dioxide and chlorides. Cem Concr Compos 2002;24:45–53.
[20] Caballero CE, Sanchez E, Cano U, Gonzalez JG, Castano V. On the effect of fly ash on the corrosion properties of reinforced mortars. Corros Rev 2000;18:105–12.
[21] Montemor MF, Simoes AMP, Salta MM. Effect of fly ash on concrete reinforcement corrosion studied by EIS. Cem Concr Compos 2000;22:175–85.
[22] Payá J, Monzó J, Borrachero MV, Peris-Mora E. Mechanical treatment of fly ashes. Part I. – physico-chemical characterization of ground fly ashes. Cem Concr Res 1995;25:1469–79.
[23] Payá J, Monzó J, Borrachero MV, Peris-Mora E, González-Lopez E. Mechanical treatment of fly ashes. Part II: particle morphologies in ground fly ashes (GFA) and workability of GFA–cement mortars. Cem Concr Res 1996;26(2):225–35.
[24] Payá J, Monzó J, Borrachero MV, Peris-Mora E, González-López E. Mechanical treatment of fly ashes. Part III: studies on strength development of ground fly ashes (GFA)–cement mortars. Cem Concr Res 1997;27:1365–77.
[25] Payá J, Monzó J, Borrachero MV, Peris-Mora E, Amahjour F. Mechanical treatment of fly ashes Part IV: strength development of ground fly ash cement mortars cured at different temperatures. Cem Concr Res 2000;30:543–51.
[26] Payá J, Monzó J, Borrachero MV, Peris-Mora E. Comparisons among magnetic and non-magnetic fly ash fractions: strength development of cement–fly ash mortars. Waste Manag 1996;16:119–24.
[27] Choi YS, Kim JG, Lee KM. Corrosion behaviour of steel bar embedded in fly ash concrete. Corros Sci 2006;48:1733–45.
[28] UNE 80301:96. Cementos: cementos comunes. Composición, especificaciones y criterios de conformidad; 1996.
[29] Payá J, Borrachero MV, Monzó J, Peris-Mora E, Bonilla M. Long term mechanical strength behaviour in fly ash/Portland cement mortars prepared using processed ashes. J Chem Technol Biotechnol 2002;77:336–44.
[30] ASTM, E-104-71. Maintaining constant relative humidity by means of aqueous solutions; 1988.
[31] Stern M, Geary AL. A theoretical analysis of the shape of polarization curves. J Elect Soc 1957;104(1):10–56.
[32] Castellote M, Andrade C, Alonso C. Measurement of the steady and non-steady-chloride diffusion coefficients in a migration test by means of monitoring the conductivity in the anolyte chamber. Comparison with natural diffusion tests. Cem Concr Res 2001;31:1411–20.
[33] Andrade C. Calculation of chloride diffusion coefficients in concrete from ionic migration measurements. Cem Concr Res 1993;23:724–42.
[34] Andrade C, Gonzalez JA. Techniques electrochimiques qualitatives et quantitatives pour mésurer les effects des additions sur la corrosion des armatures. Silic Ind 1982;47:289–95.
[35] Garcés P, Andión LG, De la Varga I, Catalá G, Zornoza E. Corrosion of steel reinforcement in structural concrete with carbon material addition. Corros Sci 2007;49:2557–66.
[36] Zornoza E, Payá J, Garcés P. Carbonation and reinforcing steel corrosion rate of OPC/FC3R/FA mortars under accelerated conditions. Adv Cem Res 2009;21:15–22.
[37] Payá J, Monzó J, Borrachero MV, Peris-Mora E, Amahjour F. Thermogravimetric methods for determining carbon content in fly ashes. Cem Concr Res 1998;28:675–86.